To cite this article:

Xu Y., **Jin R.***, Hu L., Li B., Chen W., Shen J., Wu P., and Fang J. (2019). "Studying the mix design and investigating the photocatalytic performance of pervious concrete containing TiO_2-soaked recycled aggregates." *Journal of Cleaner Production*. In Press, accepted for publication on 11 Nov 2019.

Studying the Mix Design and Investigating the Photocatalytic Performance of Pervious Concrete Containing TiO_2-Soaked Recycled Aggregates

- The research used recycled aggregates (RAs) in pervious concrete for air purification purpose.
- RAs could absorb more nano photocatalysts.
- The study identified the optimized mix design to achieve highest pervious concrete strength.
- The optimized concentration of TiO_2 solution was identified at 0.3% in order to achieve the highest NO degradation rate at 70% for pervious concrete.
- Previous concrete showed a more durable photocatalytic performance after rain wash.

Abstract

Demolished concrete, as one main form of construction and demolition wastes, has been widely studied of being utilized as recycled aggregates (RAs) in new concrete production. However, existing studies of applying RAs have been limited to the mechanical and durability issues of cementitious composites containing RAs. There has not been sufficient research of adopting RAs in cementitious products to also address the environmental sustainability. On the other hand, existing research utilizing cementitious products (e.g., concrete pavement) for air purification purpose have not adequately considered RA usage. Aiming to address the two sustainable objectives (i.e., waste diversion and air purification) simultaneously in concrete mix, this research adopted a two-step approach. Firstly, we studied and identified the optimal mix design of pervious concrete containing TiO_2-soaked recycled coarse aggregates (RCAs) in order to achieve the higher compressive strength; secondly, we investigated the photocatalytic performance of pervious concrete containing RCAs coated with TiO_2 photocatalysts. The photocatalytic performance of pervious concrete was also tested by applying a 10-min heavy rainwater wash. Experimental test results revealed that the internal voids of adhered mortar enabled RCAs to absorb more TiO_2 particles. The NO degradation rate of TiO_2-soaked RCAs increased from 71.4% to 80.6% when RCAs' size decreased from 15-20 mm to 5-10 mm. The orthogonal experimental investigation indicated that water-to-binder ratio had the most significant effect on concrete compressive strength, followed by ratio of RCAs to binder, and replacement ratio of RCAs to natural aggregates. The optimized mix design for pervious concrete containing RCAs was identified to achieve highest strength (i.e., water-to-binder ratio at 0.35, coarse aggregate-to-binder ratio of 3 by mass, fly ash replacement rate to Portland cement at 5%, and 50% replacement ratio of RCAs to NCAs,). The concentration of TiO_2 solution at 0.3% was identified as the optimal ratio to achieve the highest NO degradation rate at 70% before rainwater wash. The NO degradation rates of pervious concrete still reached nearly 50% after 10-min heavy rainwater wash, indicating that pervious concrete using RCAs coated with TiO_2 could largely maintain its photocatalytic capacity. This study addresses two main social and environmental issues in developing countries (e.g., China), namely overwhelming amount of construction & demolition wastes being generated, and air pollution. It leads to the cleaner production in concrete pavement construction by achieving the optimization between waste reuse, air purification, and engineering properties of porous concrete.

Keywords: Pervious concrete; recycled aggregate concrete; photocatalytic effects; mechanical properties; recycled aggregate; titanium dioxide

1. Introduction

Concrete is the most widely consumed building material, and the production of concrete is causing wide sustainability concern due to its consumption of natural resources (Mobasher, 2008). Concrete itself accounts for 50% to 70% of construction and demolition (C&D) wastes worldwide (Kim and Kim, 2007; Tam, 2008). Developing countries such as China is generating more C&D wastes due to its infrastructure development and urbanization (Jin *et al.*, 2018a; Shi *et al.*, 2016). The urgency of reducing the landfill demand in developing economies like China asks the sustainable treatment of C&D wastes (Jin *et al.*, 2017). The possibility of recycling construction wastes, particularly concrete, has become a major issue worldwide (Xiao *et al*., 2015). Recycling old concrete as aggregates for new concrete production (i.e., recycled aggregate concrete) is one of the effective approaches to achieve sustainable concrete (Xiao *et al*., 2015). Numerous studies have investigated how the recycled aggregate (RA) affected the properties of concrete containing recycled ingredients (e.g., RA), including mechanical properties (Koenders *et al*., 2014; Xiao *et al*., 2005) and durability (Beauchemin *et al*., 2018; Levy and Helene, 2004). However, there has not been sufficient research focusing on utilizing RAs in concrete for further sustainable applications, such as exploring using RAC in air purification purpose by adopting the “passive strategy” within RAC (Xu *et al*., 2018).

The increased usages of motor vehicles in countries such as China is causing the issue of deteriorating air quality. Heavy traffic causes high concentration of hazardous pollutants such as NO_x, further leading to problems in environmental deterioration and public health (Ballari *et al*., 2011; Hassan *et al*., 2010). The traditional pavement materials could not degrade air pollutants. There is a practical need to develop pavement or road materials that could purify the air. Since Fujishima and Honda (1972) who applied Titanium Dioxide (TiO_2) for photocatalytic decomposition of water, there have been several studies (Chen and Poon, 2009; Faraldos *et al*., 2016; MacPhee and Folli, 2016; Poon and Cheung, 2007; Yang, *et al*., 2017) applying TiO_2 in cementitious materials to test the photocatalytic performance. TiO_2 photocatalysis can be used in products for air purification purpose (Nakata and Fujishima, 2012) by degrading air pollution particles (e.g., NO_x). Various methods of applying TiO_2 in cementitious materials have also been described in existing studies. For example, Guo et al. (2017) applied the nano- TiO_2 in concrete surface layers using two different methods, namely intermixing and spray-coating. The mix design in the study of Guo et al. (2017) was 0.75:0.25:3.0:0.3 for Portland cement, fly ash, recycled coarse aggregates (RCAs), and water by mass. TiO_2 content on the concrete surface was 2.8% by weight, and was reduced to 2.0% after abrasion. Shen *et al*. (2015a, b) developed the photocatalytic self-cleaning concrete with its surface covered by C-S-H gel and TiO_2 layer. It was revealed that the surface of the self-cleaning concrete was covered by C-S-H and TiO_2 nano particles around tens of nm. Mahy et al. (2019) applied TiO_2 for the photocatalytic purpose on roads. It was found that the photocatalytic activity of TiO_2 reached the maximum NO degradation at 53% when the TiO_2 was coated to the concrete substrates (e.g., pavement blocks) at the loading rate between 10 and 12 g/m^2.

Pervious concrete has been utilized in various existing studies to address environmental issues, such as flooding (Kia *et al*., 2019), heat island effect (Liu *et al*., 2018), and air purification by applying TiO_2 as the photocatalytic agent (Asadi *et al*., 2014). A review of these previous studies applying TiO_2 in cementitious materials for air purification purpose reveals that: 1) most of these existing studies applied TiO_2 in conventional cementitious products (Hunger *et al*., 2010; Shen *et al*., 2015b) without utilizing RAs. However, Xu *et al*. (2018) found that RAs, due to their internal porosities, could absorb more TiO_2-based catalysts compared to natural aggregates; 2) limited studies have applied RAs in pervious concrete for air purification tests, although there have been existing standards (China Architecture & Building Press, 2016) adopting RAs in the mix design of pervious concrete; and further 3) practically, conventional concrete coated with TiO_2 may have limited durability of its photocatalytic function after being exposed to rainfalls, because TiO_2 coated to the surface of conventional concrete could easily be washed away by rainwater There have been limited studies focusing on how the photocatalytic performance of concrete pavement products could last longer, such as by introducing RAs. Extending the research of Xu *et al*. (2018), one of the novelties of this study is to utilize the features of RAs due to their internal voids which could absorb TiO_2 nano particles. The current study contributes to developing the technical approach of enhancing both the photocatalytic performance and the durability of pervious concrete containing RCAs.

This study aims to address the two main aforementioned issues in China (i.e., overwhelming amount of C&D wastes and air pollution). The objectives of this research include: 1) comparing the photocatalytic performance of RCAs and natural aggregates in different sizes when they are applied with nano-TiO_2 catalysts; 2) investigating the effects of mix design parameters on pervious concrete strength and further identifying the optimized mix design in order to achieve the highest compressive strength in pervious concrete containing RCAs; 3) identifying the optimized concentration of TiO_2 solution in terms of achieving the highest air pollutant degradation rate; and 4) exploring the photocatalytic efficiency change of pervious concrete containing TiO_2-coated RA after 10-min heavy rain wash.

2. Materials and methods

2.1. Concrete materials

Ordinary Portland cement of C42.5 Grade was used for the mixture of pervious concrete. Class II fly ash supplied by Beilun Power Plant in Ningbo China was adopted as the supplementary cementitious material. Coarse aggregates sized between 5mm and 10mm were adopted for both RCAs and natural coarse aggregates (NCAs) in this research. The selection of coarse aggregate size met the requirements of Technical Specification for Application of Pervious Recycled Aggregate Concrete (China Architecture & Building Press, 2016).The properties of coarse aggregates are listed in Table 1.

Table 1.Properties of coarse aggregate

Aggregates type	Apparent density (kg/m^3)	Bulk density (kg/m^3)	Surface dry water absorption rate (%)
RCA	1766	1115	6.4
NCA	2820	1453	0.4

Polycarboxylic acid superplasticizer with water reduction rate at 25% was applied. TiO_2 was used as the photocatalyst in this study. The 25% water reduction rate for the superplasticizer was chosen because of the high cohesiveness of recycled aggregate concrete which generally had lower slump. It was recommended to have the water reduction rate over 20%. The superplasticizer used in this study was polycarboxylate, which was convenient for the mix design of pervious concrete containing RCAs. Table 2 displays the physical properties of TiO_2.

Table 2. Properties of TiO_2

Appearance	White powder
Crystal structure	Mischcrystal TiO_2 (approximately 75% of Anatase and 25% of Rutile)
TiO_2 Content	>96
Photocatalytic efficiency	≥68

2.2. Preparation of TiO_2-based photocatalysts

The TiO_2 concentration at 0.3% was adopted by Yang *et al*. (2017) for the photocatalytic depollution test. However, the ideal or optimized TiO_2 concentration was not identified. As a step forward from the study of Yang *et al*. (2017), the TiO_2 solution with concentration up to 0.6% was prepared by ultrasonically dispersing TiO_2 powders into distilled water. RCAs were soaked in the solution for 24 hours and then removed to be dried under the controlled temperature of

105°C. Fig. 1 shows the TiO_2 solution and recycled coarse aggregates (RCAs) soaked with TiO_2.

(a) TiO_2 solution with concentration at 0.6%   (b) RCAs soaked with TiO_2

Fig. 1. Preparation of RCAs soaked with TiO_2

After obtaining RCAs soaked with TiO_2, the method of aggregates coated with cement pastes described by Ping and Beaudoin (1992) was followed to produce pervious concrete containing TiO_2-soaked RCAs. Fig. 2 describes the detailed steps of pervious concrete preparation.

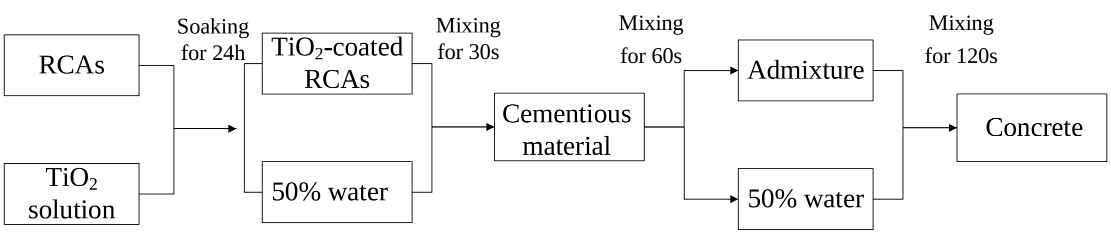

Fig.2. Workflow of preparing pervious concrete containing TiO_2-soaked RCAs

According to Fig. 2 and following the mix design procedure, RCAs were initially immersed in theTiO_2 solution to obtain the TiO_2-soaked RCAs for later concrete mixing. Then the natural aggregates, 50% of the mixture water, and TiO_2-coated RCAs were added into the mixer. The mixing time was 30s in order to have the aggregates uniformly wetted. Then the cementitious materials were added to the mixer for another 60s' mixing in order to have the binder materials wrapping the aggregate surface. Finally, the remaining 50% of the mixture water and the superplasticizer were added to the mixer for another two minutes' mixing.

2.3. Orthogonal arrays and Taguchi method

The orthogonal array design adopting the Taguchi method (ReliaSoft, 2012) was adopted as the statistical approach to identify the optimal mix design of pervious concrete according to the compressive strength. Taguchi method, also known as orthogonal array design method, is a broadly accepted method in design of experiment, which has proven in producing high-quality outputs at subsequently low cost (Davis and John, 2018). The Taguchi Orthogonal Array is a highly fractional orthogonal design based on a design matrix and allows the selection of subset of combinations of multiple factors at multiple levels (ReliaSoft, 2012), for example, replacement ratio of fly ash to Portland cement (FA%), the replacement ratio of RCAs to NCAs (RCA%), and water-to-binder (*w/b*) ratio in this study. The experiments required to complete this statistical test is relatively small, such as nine experimental groups in this study. The Taguichi Orthogonal Array method, generally based on uniformly distributed datasets, can be combined with range analysis and analysis of variance (ANOVA) to evaluate the significance of the effect of each independent variable on the dependent variable. More detailed descriptions and steps to conduct the Taguchi method can be found in Koschan and Antony (2006).

Following the Technical Specification for Application of Pervious Recycled Aggregate Concrete (China Architecture & Building Press, 2016), the compressive strength of pervious concrete should not be lower than 20 MPa. The compressive strength of pervious concrete should be considered of fundamental importance before conducting further photocatalytic environmental tests. In this study, the orthogonal array design was only applied in determining the optimal mix design to achieve the required compressive strength before conducting the further photocatalytic tests.

The key to orthogonal design is the selection of the orthogonal table. The orthogonal table is denoted as $L_n(a^p)$, where *L* represents an orthogonal table; *n* denotes the number of rows in the table, which is also the number of experimental sets; *p* is the number of columns in the orthogonal table, which is also the maximum number of factors that can be arranged in the table; *a* indicates the number of levels taken by each factor. In this study, the orthogonal table consisting of four factors and three levels denoted as L_9 (3^4) was defined. The four factors of *w/b* ratio, coarse aggregate-to-binder ratio, FA%, and RCA% were selected. These three levels and four factors are shown in Table 5.

2.4. Test facilities

The compressive strength of concrete specimen in this study was tested following *Standard for Test Method of Mechanical Properties on Ordinary Concrete* (2002). The cubes with dimensions of 100 mm ×100 mm×100 mm were prepared for the compressive strength test, with the loading rate at 0.4 MPa/s. The permeability coefficient of pervious concrete was tested following *Technical Specification for Pervious Cement Concrete Pavement* (2009). The detailed test procedure is described in the following steps: (1) placing the concrete specimen in the vacuum barrel, evacuating it to reach the pressure of (90±1) kPa, and keeping it for 30 minutes; (2) adding water to the vacuum barrel to make the water level higher than the specimen by 100 mm; and (3) stopping vacuuming for 20 minutes and removing the sample from the vacuuming barrel. Afterwards, following the schematic diagram illustrated in Fig. 3, the test specimen (denoted as 5 in Fig. 3) is placed in the cylinder (i.e., 8). The frame denoted as 4 in Fig. 3 is placed in the overflow water tank (i.e., 3). Then the water inlet (i.e., 1) is opened. The water flows through the cylinder (i.e., 8) and passes through the pervious concrete specimen (i.e., 5) into the overflow flume (i.e., 3) until water in the cylinder (i.e., 8) starts being discharged through the overflow pipe (i.e., 2). The water inflow amount is then adjusted to balance the water inlet (i.e., 1) and the overflow pipe (i.e., 2), Finally, the water amount (denoted as Q) in the graduated cylinder (i.e., 6) and the water-head difference (denoted as h) in the steady period are recorded. The temperature (denoted as T) at the same time is also recorded.

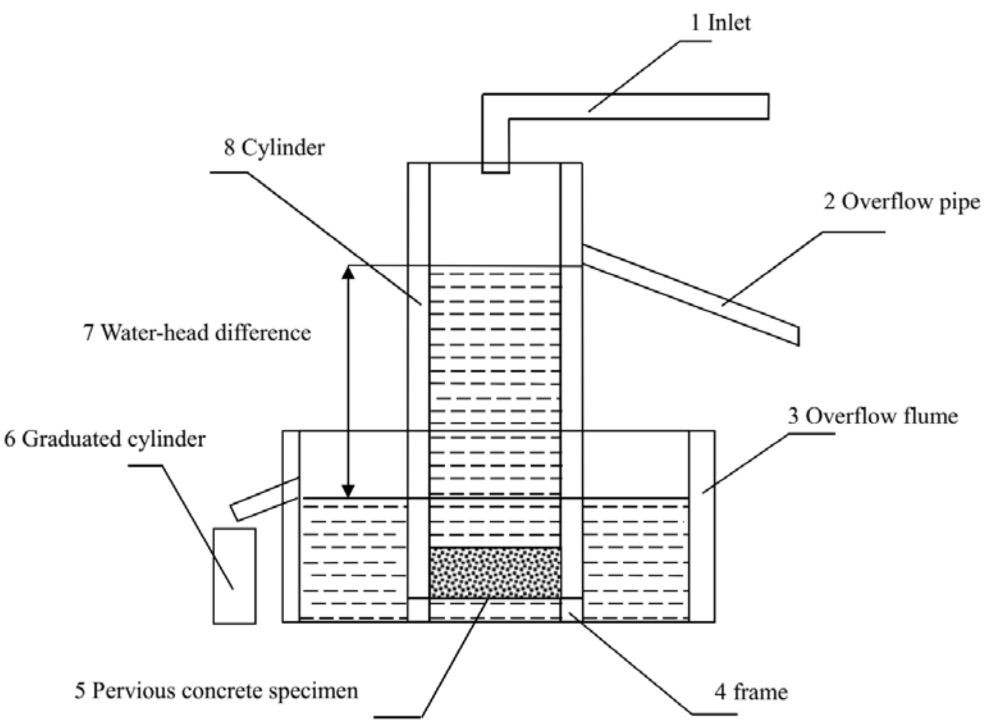

Fig.3. Schematic diagram for the test of permeability coefficient of pervious concrete

The water permeability coefficient is then calculated according to Equation (1),

$$K_T = \frac{Q_1 \times L}{A \times h \times t} \quad \text{Equation (1)}$$

where K_T means the water permeability coefficient at water temperature of T; Q_1 denotes the water amount flowing through the pervious concrete specimen by the time interval of t; L is the thickness of the permeable concrete specimen; and A is the cross-sectional area of the specimen.

The microstructure of pervious concrete was observed using Phenom Pro as the desktop SEM (i.e., scanning electron microscope).

The schematic diagram of the laboratory setup to measure NO degradation by applying the TiO_2-coated pervious concrete is demonstrated in Fig.4.

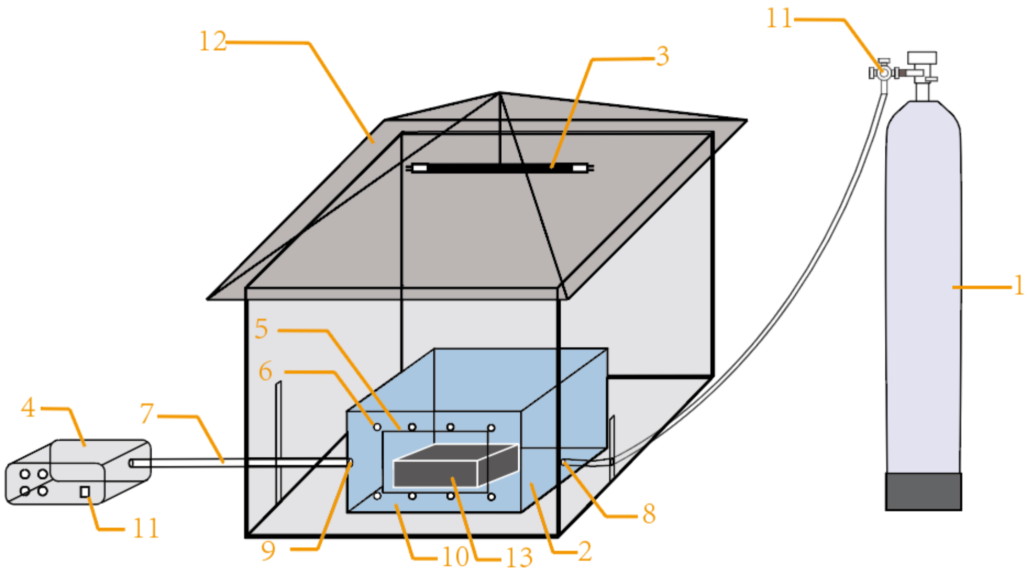

1: Gas supply source; 2: Reactor; 3: UV light source; 4: Exhaust analyzer; 5: Rubber ring; 6: Screws; 7: Airway; 8: Air inlet; 9: Air outlet; 10: Transparent gate; 11: Valve; 12: Reflective sheltering; 13: specimen

Fig.4. Schematic diagram of experimental test facility to measure NO degradation

Following *Test Method of Photocatalytic Materials for Air Purification* (2009), the test facility for the experimental measurements of NO degradation was prepared as shown in Fig.5. The photocatalytic tests of degrading NO were performed following *Measurement Method for Photolysis Performance Index of Photocatalytic Nano-Materials* (2013).

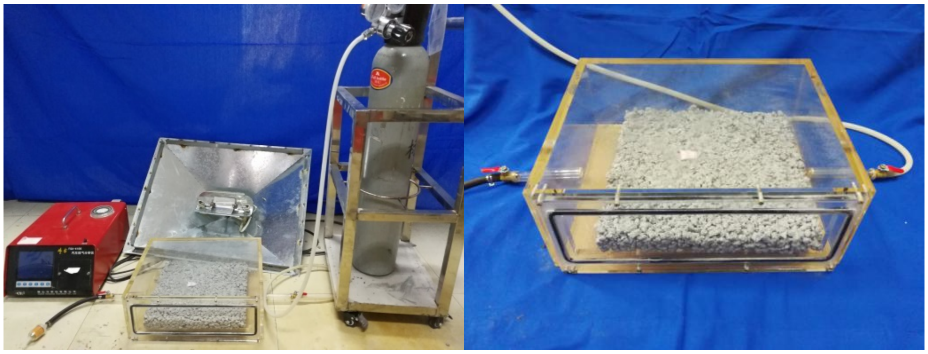

Fig.5. Experimental tests of applying pervious concrete specimen containing TiO_2-coated RCAs to degrade NO

The test facility shown in Fig.5 mainly consists of NO cylinder, reactor, UV light source, the iron-made cubic box, and exhaust gas analyzer using the FGA-4100 mode.. The parameters of the exhaust gas analyzer is displayed in Table 3.

Table 3. Parameters of FGA-4100 mode exhaust gas analyzer

Gas for test	HC	CO	CO_2 (%)	O_2 (%)	NO_x(ppm)
Test method	Spectrophotometric Infrared Absorption Method			Principle of electrochemistry	
Measuring range	0-12000	0-10	0-20	0-25	0-400
Resolution ratio	1	0.01	0.1	0.1	1
Drift range /h	±4	±0.02	±0.2	±0.2	

The iron-made cubic box was manufactured as the sheltering device to prevent natural lighting coming into the reactor. The exhaust gas analyzer was used to test the NO degradation. The NO degradation rate was calculated using Equation (2):

$$NO\ Degradation\ Rate = \frac{Initial\ concentration\ of\ NO - Final\ concentration}{Initial\ concentration}$$

Equation (2)

The experimental procedure based on Fig. 5 and schematic diagram shown in Fig.4 is described in the following six steps: (1) placing the concrete specimen in the reactor, tightening the sealing screw, and checking the air tightness; (2) opening the outlet value and the intake valve in the reactor, opening the air pump of exhaust gas analyzer, and discharging the gas in the reactor, the intake pipe, and the outlet pipe; (3) closing the air pump when the gas concentration becomes constant in the exhaust gas analyzer; (4) opening the valve of the NO cylinder, adjusting the size of the cylinder valve, observing the change of NO concentration on the exhaust gas analyzer and waiting for the NO concentration to stay unchanged, recording the initial concentration value, and then turning on the UV light source at the top of the iron-made cubic box; (5) recording the NO concentration change on the exhaust gas analyzer once every three minutes until the NO concentration remains unchanged within nine minutes; and (6) recording the final concentration value, turning off the light source, and closing the NO cylinder value.

It should be noticed from Fig.4 and Fig.5 that the pervious concrete specimens under tests were with the four sides unsealed. Several previous studies on the photocatalytic performance of concrete specimens (e.g., Lee et al., 2014; Wang et al., 2015; and Xu et al., 2018) were also found without the four sides of concrete specimens sealed to eliminate the effects from side surfaces which could also be exposed to lighting. The experimental procedure was designed with four sides of concrete specimens unsealed so as to allow the comparison between this study and these prior studies in terms of the photocatalytic performance. As seen in Fig.4 and Fig.5, the confined space with an inside UV light source could allow mainly the top surface of the concrete specimen exposed to UV light, whilst the four sides of surfaces would have significantly lower exposure to UV light. Recognizing the limitation regarding the four sides of specimens unsealed, future work could test the side effects by also sealing the four sides of pervious concrete specimens for photocatalytic experiments.

2.5. Experimental study of pervious concrete exposed to rain wash

It is known that the pavement’s photocatalytic performance will be diminished when exposed to outdoor adverse conditions such as rainwater wash. The TiO_2 particles attached to the surface of aggregates can easily move to the concrete surface. Under adverse outdoor weather condition (e.g., heavy rain), these TiO_2 nano particles could be washed away by rain, causing the loss or reduced photocatalytic effect of concrete products. The experimental work was designed in this study to investigate the photocatalytic performance reduction of pervious concrete containing TiO_2-coated RCAs. Fig. 6 and Fig. 7 display the schematic diagram and the facility of applying rainwater to wash pervious concrete.

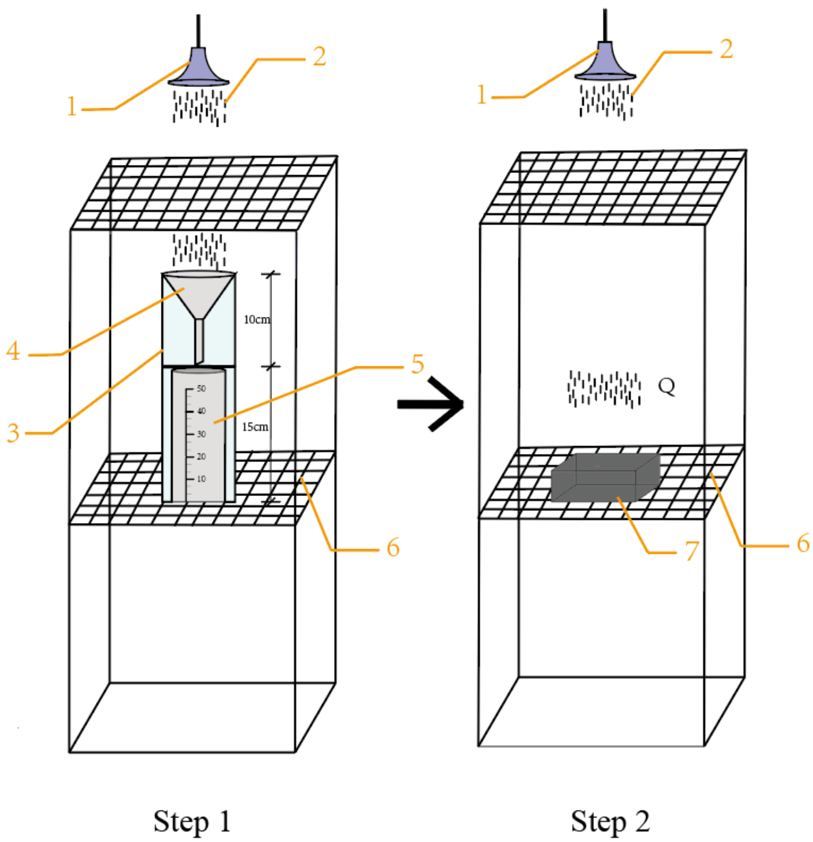

1: Sprinkler; 2: Rainwater flow; 3: Rainwater gauge; 4: Funnel; 5: Volumetric cylinder; 6: Permeable mesh; 7: Concrete specimen

Fig.6. Schematic diagram of rainwater wash facility for the test of pervious concrete

(a) Rain gauge (b) Facility for rain wash

Fig.7. Rain wash facility for the experimental study of pervious concrete

The rain gauge (Model No. J16022) is a tool for measuring the rainfall. It consists of rain inlet, a funnel, a water storage tank, and the specialized measuring cup. It was placed in the rainfall experimental test site. The rainwater fell into the rain inlet and was collected by the storage tank through the funnel. After the rainfall stopped, the water in the storage tank was measured in the measuring cup. The experimental precipitation was set at 25 cm per day or equivalent to 10.4 mm/hour, which is considered heavy storm according to United States Geological Survey (2018). The pervious concrete specimens, with surface area dimension of 300mm by 300mm and thickness of 50 mm, received the precipitation of 6 cm^3 in 10 minutes during the experiment. Adopting this precipitation rate, the NO degradation rates before and after rainwater wash were obtained to measure the deterioration of photocatalytic performance of pervious concrete. The simulation of heavy storm rainfall for each test specimen was controlled at 10 min to ensure that all tests were under the same rainfall conditions. The 10-min period is considered reasonable in simulating the real-life heavy storm, which is generally with high intensity of rainfall but in a short period. Actually, the real-life heavy storm may be with a non-uniform pattern and unrealistic for comparative studies of different concrete specimens. Therefore, the current experimental setup for the rainfall test is considered realistic for studying the photocatalytic performance change of pervious concrete with different concentrations of TiO_2.

3. Results

3.1. Photocatalytic performance of RCAs coated with TiO_2

Using the desktop SEM, the nano TiO_2 particles attached into the voids of RCAs were observed as shown in Fig. 8.

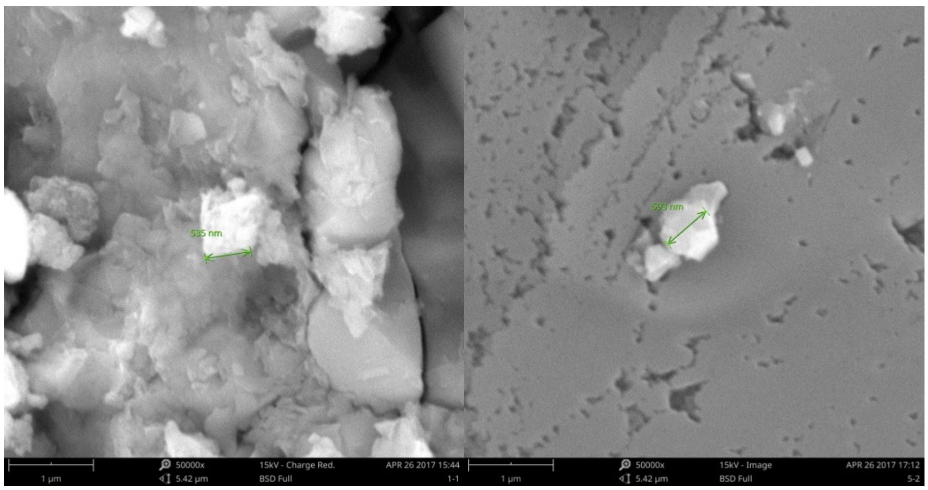

Fig.8. Microstructure of observing TiO_2 particles absorbed into the internal voids of RCAs (Scale at 50,000:1).

Fig.8 captured TiO_2 particles attached to RCAs' voids from different angles and locations within pervious concrete. As can be seen in Fig.8, the porous mortar attached to the surface of RCAs could absorb nano TiO_2 particles after soaking RCAs into TiO_2 solution and drying them.

This research started by comparing the photocatalytic performance between RCAs and NCAs. As shown in Fig.9 and Fig.10, NCAs and RCAs with three different sizes (i.e., 15-20 mm, 10-15 mm, and 5-10 mm) were obtained to test their NO degradation performance.

(a) (b) (c)

Fig.9. RCA sized at (a)15-20 mm, (b) 10-15 mm, (c) 5-10 mm

(a) (b) (c)

Fig.10. NCA sized at (a) 15-20 mm, (b) 10-15 mm, (c) 5-10 mm

Following the procedure described in Section 2.2, these six different types of coarse aggregates were soaked in TiO_2 solution with the concentration at 0.6%.

The photocatalytic experimental facility described in Figs. 5 and 7 was applied to each type of TiO_2-soaked aggregate to test the NO degradation rates. Table 4 lists and compares the NO degradation performance between NCAs and RCAs.

Table 4. Comparison of photocatalytic performance between RCAs and NCAs

Aggregate size	**5-10 mm**	**10-15 mm**	**15-20 mm**
RCA	80.6%	74.4%	71.4%
NCA	66.6%	67.7%	62.3%

It can be seen from Table 4 that both RCAs and NCAs coated with TiO_2 could degrade NO.

However, RCAs outperformed NCAs in its photocatalytic reaction. The superior performance of RCAs was mainly due to two reasons. Firstly, the internal voids of RCAs could store TiO_2 to allow more photocatalytic reactions. Secondly, TiO_2 can be more easily loaded into RCAs surface because of mortar attached to its surface as shown in Fig.9. NCAs, in comparison, have a less rough surface and are hence more difficult to have TiO_2 attached to them. Further comparing the photocatalytic performance of the same type of aggregate with different sizes reveal more findings. TiO_2 could be absorbed either into the internal voids or surface of RCAs. RCAs with smaller sizes would have more internal porosities and higher specific surface area to absorb more TiO_2. Therefore, as the size of RCAs increases, the photocatalytic performance would decrease due to the reduced internal porosities and lower specific surface area. Different from RCAs, NCAs have little internal porosity. The TiO_2 particles could only be attached to the surface of NCAs, hence the effects of NA size on the photocatalytic performance turned out less significant. As seen in Table 4, the photocatalytic performance for NCAs sized between 5-10mm and 10-15mm was least significant, although there was a minor reduction of photocatalytic performance when the NCA size reached 15-20 mm.

3.2. Mix design of pervious concrete adopting RCAs

According to *Technical Specification for Application of Pervious Recycled Aggregate Concrete* (China Architecture & Building Press, 2016), the replacement ratio of RCAs to NCAs (RCA%) should not be lower than 30%, water-to-binder (*w/b*) ratio should be between 0.25 and 0.35, and the replacement ratio of fly ash to Portland cement (FA%) should not be higher than 30%. The w/b ratio and coarse aggregate-to-binder ratio (*a/b*) are considered critical factors affecting the mechanical properties of pervious concrete (Shi et al., 2016). Therefore, the four factors (i.e., RCA%, *w/b*, FA%, and *a/b*) were decided. Following the orthogonal table in the form of L_9 (3^4) , three levels were confirmed for the four factors. Further based on the researchers' own prior trials, the levels for each factor shown in Table 5 were determined by the research team. For example, should not be lower than 0.27 to maintain the workability of pervious concrete containing RCAs.

Table 5. Parameters defined in the orthogonal experimental design

Level	**Independant variables**			
	(A) *w/b*	**(B) *a/b***	**(C) FA%**	**(D) RCA%**
(a)	0.27	3	5%	30%
(b)	0.3	3.3	10%	50%
(c)	0.35	4	20%	70%

Based on the orthogonal design defined in Table 5, nine experimental tests were performed covering different combinations of these four independent variables. The compressive strength and photocatalytic performance measured by NO degradation rates were tested and summarized in Table 6.

Table 6.Experimental arrangement and range analysis for comprehensive strength of pervious concrete

Experiment No.	**(A)** ***w/b***	**(B)** ***a/b***	**(C)** **FA%**	**(D)** **RCA%**	**Index** Compressive strength (MPa)	NO Degradation rate
1#	0.27(a)	3(a)	5%(a)	30%(a)	9.0	47%
2#	0.27(a)	3.3(b)	10%(b)	50%(b)	6.8	62%
3#	0.27(a)	4(c)	20%(c)	70%(c)	2.2	38%
4#	0.3(b)	3(a)	10%(b)	70%(c)	7.1	14%
5#	0.3(b)	3.3(b)	20%(c)	30%(a)	4.4	18%
6#	0.3(b)	4(c)	5%(a)	50%(b)	7.4	52%
7#	0.35(c)	3(a)	20%(c)	50%(b)	19.8	33%
8#	0.35(c)	3.3(b)	5%(a)	70%(c)	13.8	10%
9#	0.35(c)	4(c)	10%(b)	30%(a)	9.2	17%
Range Analysis	**Index**	**Index**	**Index**	**Index**	–––	–––
K_I	6.000	11.967	10.067	7.533		
K_{II}	6.300	8.333	7.700	11.333		

K_{III}	14.267	6.267	8.800	7.700		
Y	8.267	5.700	2.367	3.800		

The range analysis of orthogonal test was performed following the procedure described in Xu (2015). In Table 6, Ki denotes the average comprehensive strength for a certain variable at Level i (e.g., *I*, *II*, or *III*). By comparing and evaluating the index values (i.e., compressive strength) at Ki, the optimal level of variables can be confirmed. The parameter *Y*, as shown in Table 6, is computed following Equation (3),

$$\text{Y (MPa)} = \max\{K_{\mathrm{I}}, K_{\mathrm{II}}, K_{\mathrm{III}}\} - \min\{K_{\mathrm{I}}, K_{\mathrm{II}}, K_{\mathrm{III}}\} \qquad \text{Equation (3)}$$

The parameter *Y* shows the effect of variables on the compressive strength. A high *Y* value of corresponding to a certain variable (e.g, *w/b*) means that this variable has a relatively strong effect on the compressive strength. The significance of each independent variable on the compressive strength was tested using ANOVA (i.e., analysis of variance) as shown in Table 7. The three different key threshold values (i.e., K_I, K_{II}, and K_{III}) linked to the different variables are displayed in Figs.11-13.

Following the experimental data collected in Table 6, a *F*-test based on ANOVA was performed to evaluate the impact of each independent variable on the compressive strength of pervious concrete. As displayed in Table 7, the related *F* value is a key parameter of ANOVA. The *F* value was computed following Equation (4),

$$F = \frac{S_A / f_A}{S_e / f_e} \qquad \text{Equation (4)}$$

where S_A denotes the sum of squared deviations of factors; f_A is the degree of freedom of factors; S_e is the sum of squared deviations of experimental errors; and f_e means the degree of freedom of experimental errors. Using the *F*-test to evaluate the effects of independent mix design variables on concrete strength can be found in several existing studies (e.g., Jin *et al.*, 2018b).

The null hypothesis was that the given independent variable did not have a significant effect on pervious concrete strength. The null hypothesis would be declined if the obtained *F* value is equal to or higher than the critical *F* value at defined levels of significance (i.e., 0.05, 0.1, and 0.25 in Table 7). A higher *F* value would indicate that the given independent variable had a more significant impact on the compressive strength of pervious concrete.

Table 7. ANOVA for comprehensive strength

Indepen-dent variable	**Sum of squares**	**Degrees of freedom**	**Variance**	***F* value**	***p* value**	***F* value at defined level of significance**	**Evaluation of significance**
w/b	131.6792	2	65.84	15.74	0.01		Most significant
						$F_{0.05}(2,4)=6.94$	
a/b	49.9832	2	24.99	5.97	0.06		Significant
						$F_{0.1}(2,4)=4.32$	
RCA%	27.7152	2	13.86	3.31	0.14		Less significant
						$F_{0.25}(2,4)=2.00$	
FA%	8.3672	2	4.184	1.00			Least significant
Error	8.3672	2	4.18				
Correc-tion Error	16.7344	4	4.18				
Total	226.112						

As seen in Table 7, there are three threshold *F* values corresponding to the three different levels of significance. The three different threshold values define the significance of each independent variable in one of the four different categories (i.e., “most significant” if the *F* value is higher than 6.94; “significant” if the computed *F* value is between 4.32 and 6.94; “less significant” if the *F* value is between 2.00 and 4.32; and “least significant” if the *F* value is lower than 2.00. It can be seen from Table 7 that *w/b* (i.e., water-to-binder) ratio has the highest impact on concrete strength, followed by *a/b* (i.e., aggregate-to-binder ratio), replacement ratio of RCAs, and fly ash percentage. As seen in Fig. 11, the compressive strength of pervious concrete on Day 28 increased with *w/b* ratio.

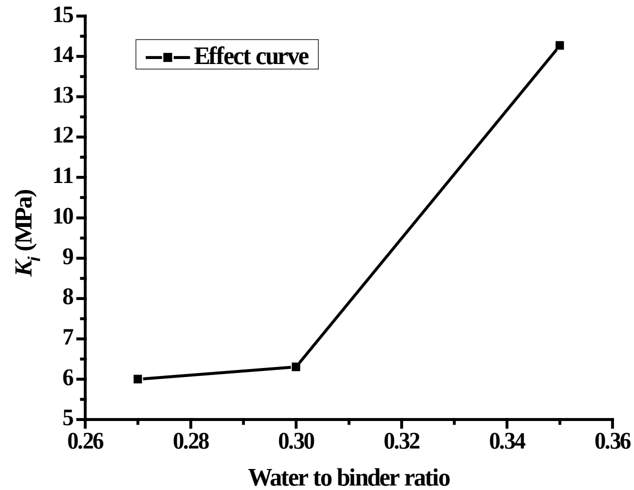

Note: the definition of K_i in Figs.11-13 is consistent with what has been defined in Table 6.

Fig. 11. 28-day compressive strength of pervious concrete at different *w/b* ratios

The trend of compressive strength change with *w/b* ratio in pervious concrete turned out different compared to that in conventional concrete due to the fact that the strength growth in pervious concrete does not follow Bolomey's equation (Bolomey, 1927). Instead, pervious concrete is designed to have voids to allow moisture to permeate through it. The higher porosity within pervious concrete causes strength reduction. The strength developed within pervious concrete is based on contact points connected within its internal structure and the bonding strength at connections (Zhong and Wille, 2016). Pervious concrete produced in this research was based on the method of coating aggregates with cement paste (Ping and Beaudoin, 1992). A lower *w/b* ratio would cause insufficient hydration of cementitious materials, leading to lower bonding strength at connections. RCAs would absorb more moisture than NCAs in this study, causing inadequate hydration of cementitious materials at contact point connections and resulting in lower strength developed.

The effect of *a/b* ratio on concrete compressive strength is shown in Fig. 12. A negative relationship between *a/b* ratio and compressive strength can be observed. As indicated in Fig.12, when *a/b* ratio is higher than 4.0, there would be insufficient cementitious materials covering aggregate surfaces, causing their inadequate hydration which further leads to lower bonding strength at contact points.

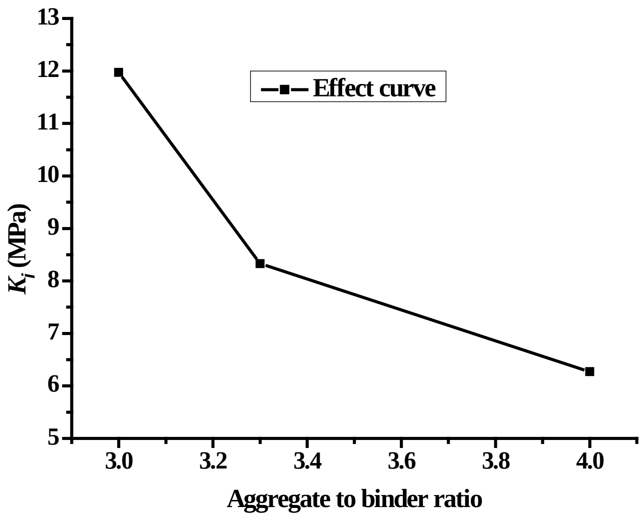

Fig.12. 28-day compressive strength of pervious concrete at different *a/b* ratios

The effect of RCA% (i.e., replacement ratio of RCAs to NCAs) on concrete strength is illustrated in Fig. 13. It is seen in Fig. 13 that the compressive strength of pervious concrete would first increase with RA% until it reaches 50%, and then decrease as RA% continues increasing.

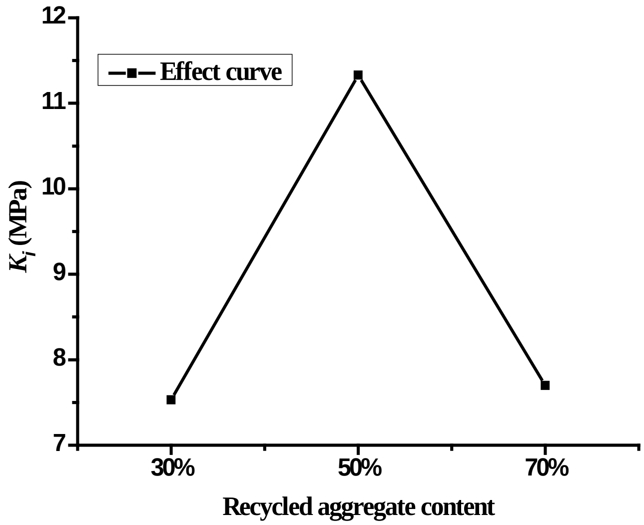

Fig. 13. 28-day compressive strength of pervious concrete at different replacement ratios of RCAs

Consistent to the earlier study performed by Jin *et al*. (2018a), Xu and Sun (2011), and Xu *et al*. (2018), lower replacement ratios of RCAs could increase the concrete strength due to the fact that RAs had their positive effects (e.g., internal curing) in developing concrete strength. This positive effect of RAs on concrete strength was not affected by adding TiO_2 particles (Xu and Sun, 2011). However, as the RA replacement ratio increases, the negative effects of RAs would outweigh their positive impacts, due to RA's lower quality in terms of their physical properties and weak interfacial transition zones identified by earlier studies (Lei *et al*., 2018; Li *et al*., 2017; Limbachiya *et al*., 2000). As a result, a higher percentage (i.e., over 50%) of RCAs replacing NCAs would decrease concrete strength.

The optimized mix design for pervious concrete containing TiO_2-coated RCAs is therefore identified in order to achieve the highest compressive strength. Table 8 lists the optimized mix design.

Table 8. Optimized mix design of pervious concrete in this study

w/b	*a/b*	FA%	RCA%	Compressive strength on Day 28 (MPa)	Water permeation coefficient (mm/s)	NO degradation rate (%)
0.35	3	5%	50%	21.6	12.5	37.4

3.3. Effects of TiO_2 concentration on NO degradation rates of photocatalytic pervious concrete

The optimized mix design parameters identified in Table 8 were then adopted to produce pervious concrete with RCAs containing nano particles from different concentrations of TiO_2 solution. The photocatalytic performance in terms of NO degradation rates were tested and measured both before and after the 10-min heavy rainwater wash adopting the precipitation rate described in Section 2.5. Six different concentrations (i.e., 0%, 0.1%, 0.2%,0.3%, 0.4%, and 0.5%) of TiO_2 solution were studied in order to identify the optimized concentration for achieving the highest photocatalytic performance. Data collected from photocatalytic tests are summarized in Table 9.

Table 9. Photocatalytic performance of pervious concrete containing RCAs soaked at different concentrations of TiO_2 solution

Test No.	TiO_2 solution concentration	NO degradation rate before rainwater wash	NO degradation rate after 10-min rainwater wash
T-0	0	0	0
T-1	0.1%	61.4%	40%
T-2	0.2%	63.6%	44.30%
T-3	0.3%	70%	49.60%
T-4	0.4%	52.2%	41.50%
T-5	0.5%	42.2%	31.10%

The highest NO degradation rate was achieved at 70%. Compared to the photocatalytic performance of concrete specimens containing TiO_2 nano particles in some previous studies, e.g., NO degradation rate at 17.6% in Xu et al. (2018), 32%-56% in Mahy et al. (2019), and 62% in Yang et al. (2019), this study achieved the highest NO degradation rate by adopting TiO_2-soaked RCAs in the mix design of pervious concrete.

It is also indicated from Table 9 that the photocatalytic performance of pervious concrete containing TiO_2-coated RCAs did not always increase with the concentration of TiO_2 solution. Instead, there was an optimized TiO_2 solution concentration identified at 0.3%. The highest NO degradation rate was achieved at 70% when 0.3% concentration of TiO_2 solution was used to soak RCAs. Compared to the photocatalytic performance of ready-mix concrete in the study of Xu *et al*. (2018) where the NO_x degradation rate was below 20%, applying TiO_2-coated RCAs could significantly increase the air pollutant degradation rate. The photocatalytic performance of pervious concrete would be decreased when the concentration of TiO_2 solution was higher than 0.3%. This could be due to the fact that the TiO_2 concentration over 0.3% decreased the permeability of pervious concrete as evidenced by the experimental tests. In this study, following the experimental test procedure illustrated in Fig.3 and Equation (1), the permeability coefficients for pervious concrete specimens with TiO_2 concentrations at 0.3%, 0.4%, and 0.5% were 15.45 mm/s, 14.78 mm/s, and 13.36 mm/s respectively. It was indicated that the increased TiO_2 concentration reduced the permeability coefficients of pervious concrete specimens, further decreasing the exposure of the photocatalytic nano-materials to UV light. As a result, the photocatalytic performance was lowered. To further validate the effects of TiO_2 concentration on pervious concrete's photocatalytic performance, the micro-structures of pervious concrete with RCAs containing TiO_2 particles from the five different concentrations of TiO_2 solution are captured in Fig. 14.

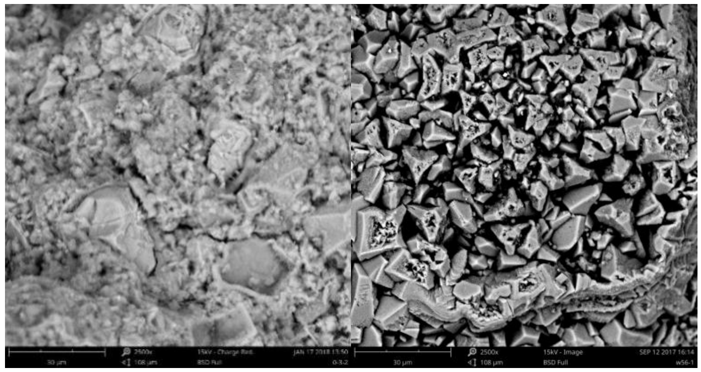

(a) Concrete microstructure observed with RCAs soaked in 0% concentration of TiO_2 solution

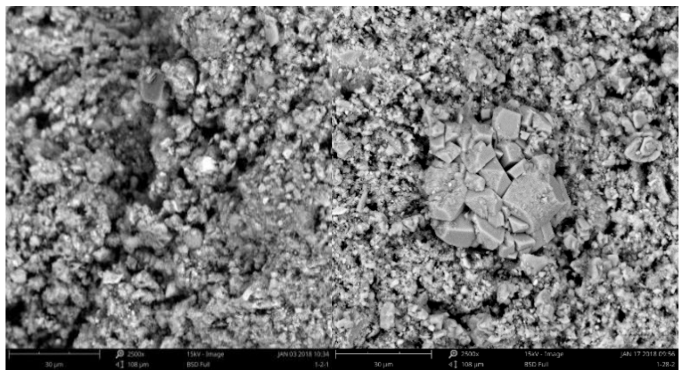

(b) Concrete microstructure observed with RCAs soaked in 0.1% concentration of TiO_2 solution

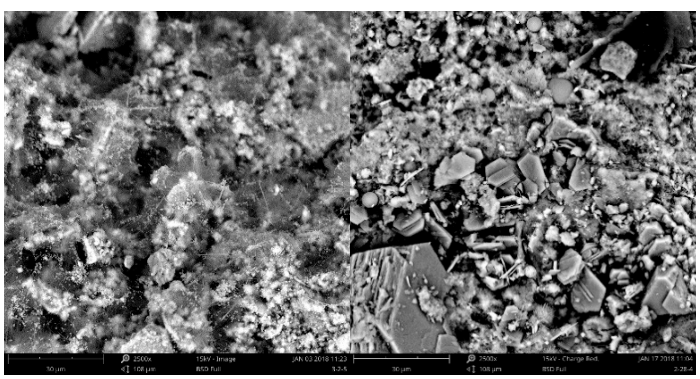

(c) Concrete microstructure observed with RCAs soaked in 0.2% concentration of TiO_2 solution

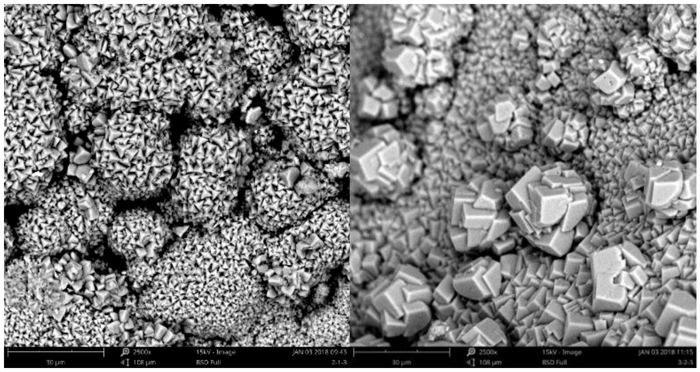

(d) Concrete microstructure observed with RCAs soaked in 0.3% concentration of TiO_2 solution

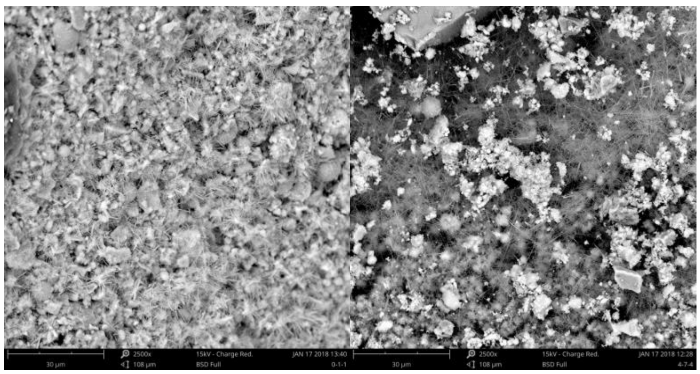

(e) Concrete microstructure observed with RCAs soaked in 0.4% concentration of TiO_2 solution

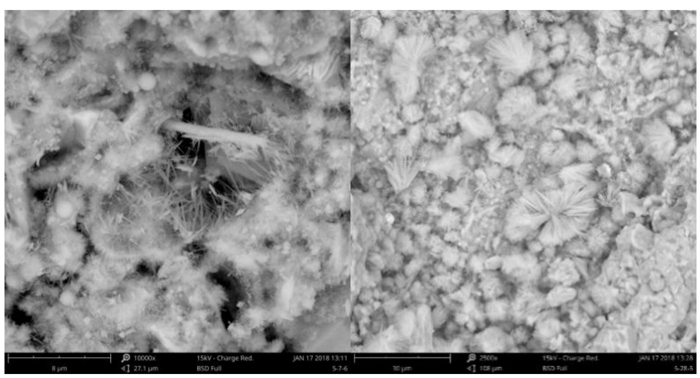

(f) Concrete microstructure observed with RCAs soaked in 0.5% concentration of TiO_2 solution

Fig. 14. Micro-structure of pervious concrete containing TiO_2-coated RCAs soaked in different concentrations of TiO_2 solution

It can be observed from Fig. 14 that when using RCAs after being soaked into 0% concentration of TiO_2 solution, the cement hydration products appeared large but not solid. According to Fig. 14-b) and c), the nano feature of TiO_2 particles formed cores during cement hydration, increasing the forming rates of cement crystals and also reducing the size of hydration products(Chandrappa and Biligiri, 2016). When the 0.3% concentration of TiO_2 solution was used to soak RCAs, TiO_2 not only accelerated the formation of dense hydration layer on cement surfaces, but also formed globular-shaped hydration product (Chen *et al*., 2011) outside the hydration layer as seen in Fig.14-c). However, as the concentration of TiO_2 solution continued increasing from 0.3%, the calcium meteorite (i.e., AFt) increased rapidly and consumed TiO_2 particles, and further reducing the photocatalytic effect of concrete.

The effect of the concentration of TiO_2 solution on cement hydration displayed in Fig. 14 can be further illustrated in Fig. 15.When the concentration of TiO_2 solution was lower than the optimized value (i.e., 0.3%), the hydration layer formed outside the cement surface. The globular hydration products would be formed when the concentration was close to 0.3%. Further increasing the concentration of TiO_2 solution would form more TiO_2-driven cores, and even create a secondary layer by connecting these cores. The calcium meteorite could also be formed as a result. It can be further seen in Fig. 14-f) and Fig.15-c) that some TiO_2-driven whiskers were formed after soaking RCAs in higher concentration of TiO_2 solution. These whiskers could be found in both the surface and inner of RCAs. RCAs could provide the internal voids to accommodate whiskers and further enhancing concrete strength growth (Xu *et al*., 2018).

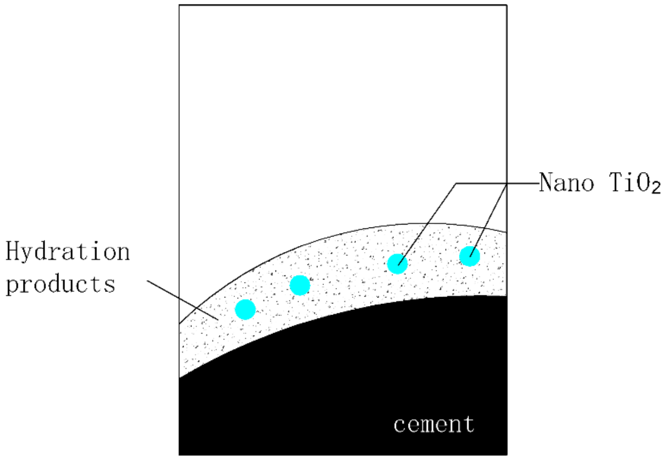

(a) Concentration of TiO2 solution lower than 0.3%

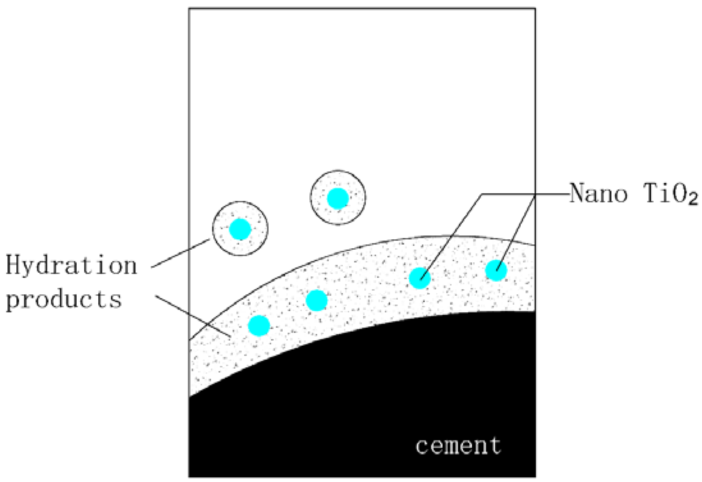

(b) Concentration of TiO2 solution at the optimized value of 0.3%

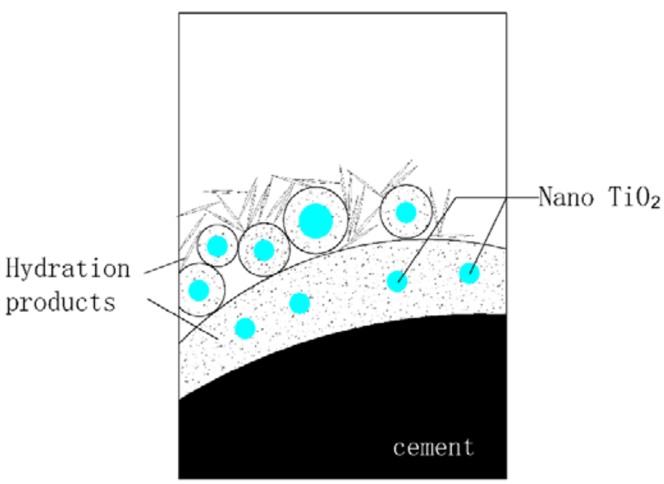

(c) Concentration of TiO2 solution higher than 0.3%

Fig. 15. Illustration of cement hydration product formation at different concentrations of TiO_2

solution

The photocatalytic performance of pervious before and after the 10-minute heavy rainwater wash was compared as seen in Fig. 16.

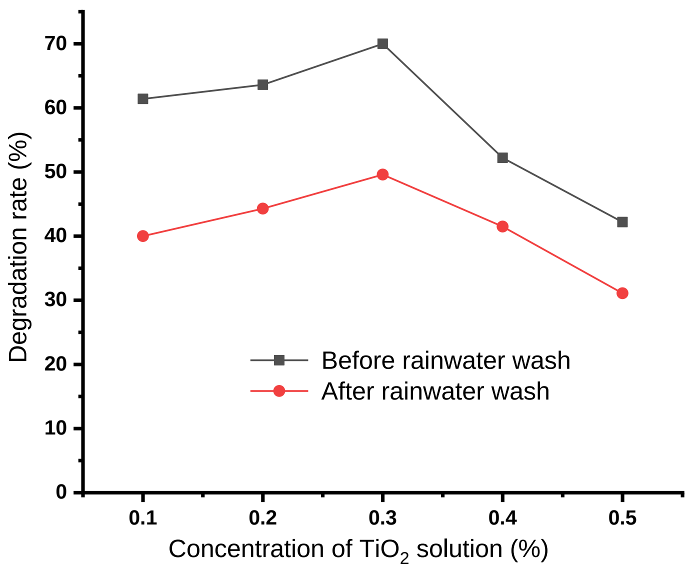

Fig. 16. NO degradation rates of pervious concrete specimens before and after 10-min heavy rainwater wash

According to Fig. 16, the photocatalytic performance of all specimens was reduced after 10-min rainwater wash, with the reduction of degradation rates of NO ranging from 20% to 35%. Rainwater wash reduced the nano TiO_2 particles. It was also found that pervious concrete with RCAs soaked in 0.3% TiO_2 solution still achieved the highest degradation rate (i.e., 49.6%) after 10-min rainwater wash.

4. Conclusion

This research focused on applying the TiO_2-soaked RCAs in pervious concrete by investigating its impacts on concrete mechanical strength as well as photocatalytic performance. The effects of nano TiO_2 particles on cement hydration were investigated through observation of concrete microstructure. Main findings are summarized below:

- Compared to NCAs, the porosity and rough surface of RCAs enabled nano TiO_2 particles being attached to them and further improved the photocatalytic effect. Smaller-sized RCAs, due to their higher specific surface area, would have better photocatalytic performance.
- The optimized mix design of pervious concrete adopting TiO_2-soaked RCAs was identified through orthogonal experimental design to achieve the highest compressive strength: water-to-binder ratio at 0.35, aggregate-to-binder ratio at 3, fly ash percentage at 5%, and the replacement ratio of RCAs to NCAs at 50%.
- RCAs were found with its positive effects on improving pervious concrete strength when its replacement ratio to NCAs were below 50%.
- Six different concentrations of TiO_2 solution were compared of their effects on the photocatalytic effects of pervious concrete. The optimized concentration was identified at 0.3% in order to achieve the highest NO degradation rate at 70%.
- Microstructure observation revealed that TiO_2 particles formed cores and enhanced the formation of globular cement hydration products when pervious concrete was produced from RCAs soaked in 0.3% TiO_2 solution. But when the concentration was higher than 0.3%, especially when reaching 0.5%, more TiO_2-driven cores and even whiskers would be formed, creating a secondary hydration layer and more calcium meteorites, the latter of which turned out reducing the concrete photocatalytic performance.
- After a 10-minute heavy rainwater wash, the pervious concrete specimens with RCAs soaked in 0.3% concentration of TiO_2 solution still displayed the highest NO degradation rate at nearly 50%, indicating a more durable photocatalytic performance.

This research addressed the gaps in applying concrete wastes for environmental protection by initiating a prototype of photocatalytic pervious concrete. RCAs were found with superior performance in absorbing photocatalysts (i.e., TiO_2) for air purification purpose. The study also addressed the issue of durability of photocatalyst concrete under rain wash from the practical perspective, indicating that applying RCAs had multiple potential advantages including reusing wastes as well as improving photocatalytic performance with better durability. The photocatalytic pervious concrete products may require higher initial cost. Preparing RAs coated with photocatalyst nano particles may also ask extra effort in the concrete mixture process. The economical, environmental, and technical aspects of the photocatalytic pervious recycled aggregate concrete need to be considered in a holistic approach.

Future research would also extend the current research in applying photocatalysts-coated RCAs in self-cleaning concrete for air purification uses. More applications of concrete members can be developed with photocatalytic functions, such as precast concrete components. It should be noticed that the application of pervious concrete containing photocatalysts-coated RCAs is not limited to air purification, but also water purification. More future studies could investigate the water purification performance of pervious concrete by utilizing RCAs coated with photocatalytic nano materials.

Acknowledgement

This research is supported by Natural Science Foundation of Ningbo (Grant No. 2018A610229) and National Natural Science Foundation of China (Grant No. 51778577). The authors would also like to acknowledge the support of Writing Retreat Fund provided by University of Brighton.

References

Asadi S., Hassan M., Kevern J.T., Rupnow T., 2014. Nitrogen oxide reduction and nitrate measurements on TiO_2 photocatalytic pervious concrete pavement. International Journal of

Pavement Research and Technology. 7(4), 273-279.

Ballari, M.M., Yu, Q.L., Brouwers, H.J.H., 2011. Experimental study of the NO and NO2 degradation by photocatalytically active concrete. Catalysis Today 161(1), 175-180.

Beauchemin, S., Fournier, B., Duchesne, J., 2018. Evaluation of the concrete prisms test method for assessing the potential alkali-aggregate reactivity of recycled concrete aggregates. Cem Concr Res 104, 25-36.

Bolomey, J., 1927. Determination of the compressive strength of mortars and concretes. Bull Tech Suisse Romande 32(5), 22-24.

Chandrappa, A.K., Biligiri, K.P., 2016. Pervious concrete as a sustainable pavement material-Research findings and future prospects: A state-of-the-art review. Constr Build Mater 111, 262-274.

Chen, J., Kou, S.C., Poon, C.S., 2011. Photocatalytic cement-based materials: Comparison of nitrogen oxides and toluene removal potentials and evaluation of self-cleaning performance. Build. Environ. 46(9), 1827-1833.

Chen, J., Poon, C.S., 2009. Photocatalytic activity of titanium dioxide modified concrete materials - Influence of utilizing recycled glass cullets as aggregates. Journal of Environmental Management 90(11), 3436-3442.

China Archicture & Building Press: Beijing, C., 2016; Volume CJJ/T 253, Technical specification for application of pervious recycled aggregate concrete.

Davis, R., John, P., 2018. Application of Taguchi-based design of experiments for industrial chemical processes. INTECH, 137-155. DOI: 10.5772/intechopen.69501.

Faraldos, M., Kropp, R., Anderson, M.A., Sobolev, K., 2016. Photocatalytic hydrophobic concrete coatings to combat air pollution. Catalysis Today 259, 228-236.

Fujishima, A., Honda, K., 1972. Electrochemical photolysis of water at a semiconductor electrode. Nature 238(5358), 37-38.

Guo, M., Ling, T.C., Poon, C.S., 2017. Photocatalytic NOx degradation of concrete surface layers intermixed and spray-coated with nano-TiO2: Influence of experimental factors. Cem Concr Compos 83, 279-289.

Hassan, M.M., Dylla, H., Mohammad, L.N., Rupnow, T., 2010. Evaluation of the durability of titanium dioxide photocatalyst coating for concrete pavement. Constr Build Mater 24(8), 1456-1461.

Hunger, M., Hüsken, G., Brouwers, H.J.H., 2010. Photocatalytic degradation of air pollutants - From modeling to large scale application. Cem Concr Res 40(2), 313-320.

Jin, R., Li, B., Zhou, T., Wanatowski, D., Piroozfar, P., 2017. An empirical study of perceptions towards construction and demolition waste recycling and reuse in China. Resour. Conserv. Recycl. 126, 86-98.

Jin, R., Li, B., Elamin, A., Wang, S., Tsioulou, O., Wanatowski, D., 2018a. Experimental Investigation of Properties of Concrete Containing Recycled Construction Wastes. International Journal of Civil Engineering. 16(11), 1621-1633.

Jin, R., Yan, L., Soboyejo, A.B.O., Huang, L., Kasal, B. 2018b. Multivariate regression models in estimating the behavior of FRP tube encased recycled aggregate concrete." Construction and Building Materials.191, 216-227.

Kia A., Wong H.S., Cheeseman C.R., 2019. High-strength clogging resistant permeable pavement. International Journal of Pavement Engineering. https://doi.org/10.1080/10298436.2019.1600693.

Kim, G.D., Kim, T.B., 2007. Development of recycling technology from waste aggregate and dust from waste concrete. Journal of Ceramic Processing Research 8(1), 82-86.

Koenders, E.A.B., Pepe, M., Martinelli, E., 2014. Compressive strength and hydration processes of concrete with recycled aggregates. Cem Concr Res 56, 203-212.

Koschan, A. and Antony, J., 2006. Taguchi or classical design of experiments: a perspective from a practitioner. *Sensor Review*.

Lee, B.Y., Jayapalan, A.R., Bergin, M.H., Kurtis, K.E., 2014. Photocatalytic cement exposed to nitrogen oxides: Effect of oxidation and binding. Cem Concr Res 60, 30-36.

Lei, B., Li, W., Tang, Z., Tam, V.W.Y., Sun, Z., 2018. Durability of recycled aggregate concrete under coupling mechanical loading and freeze-thaw cycle in salt-solution. Constr Build Mater 163, 840-849.

Levy, S.M., Helene, P., 2004. Durability of recycled aggregates concrete: A safe way to sustainable development. Cem Concr Res 34(11), 1975-1980.

Li, W., Long, C., Tam, V.W.Y., Poon, C.S., Hui Duan, W., 2017. Effects of nano-particles on failure process and microstructural properties of recycled aggregate concrete. Constr Build Mater 142, 42-50.

Limbachiya, M.C., Leelawat, T., Dhir, R.K., 2000. Use of recycled concrete aggregate in high-strength concrete. Materials and Structures/Materiaux et Constructions 33(233), 574-580.

Liu H., Luo G., Gong Y., Wei H., 2018. Mechanical properties, permeability, and freeze-thaw resistance of pervious concrete modified by waste crumb rubbers. Applied Sciences (Switzerland). 8(10), 1843.

MacPhee, D.E., Folli, A., 2016. Photocatalytic concretes - The interface between photocatalysis and cement chemistry. Cem Concr Res 85, 48-54.

Mahy, J.G., Paez, C.A., Hollevoet, J., Courard, L., Boonen, E., Lambert, S.D., 2019. Durable photocatalytic thin coatings for road applications. *Construction and Building Materials* 215, 422-434.

Measurement method for photolysis performance index of photocatalytic nano-materials, China Standard Press: Beijing, China, 2013; Volume GB/T 30452.

Mobasher, B., 2008. USA-concrete construction industry-cement based materials and civil infrastructure. CBM-CI International Workshop, Karachi, Pakistan, 73-90.

Nakata, K., and Fujishima, A. (2012). " TiO2 photocatalysis: Design and applications." *Journal of Photochemistry and Photobiology C: Photochemistry Reviews*. 13(3), 169-189.

Ping, X., Beaudoin, J.J., 1992. Modification of transition zone microstructure -silica fume coating of aggregate surfaces. Cem Concr Res 22(4), 597-604.

Poon, C.S., Cheung, E., 2007. NO removal efficiency of photocatalytic paving blocks prepared with recycled materials. Constr Build Mater 21(8), 1746-1753.

ReliaSoft, 2012. Taguchi Orthogonal Array Designs. Available via < https://www.weibull.com/hotwire/issue131/hottopics131.htm>. Accessed on 2 Feb. 2019.

Shen, W., Zhang, C., Li, Q., Zhang, W., Cao, L., Ye, J., 2015a. Preparation of titanium dioxide nano particle modified photocatalytic self-cleaning concrete. Journal of Cleaner Production 87(C), 762-765.

Shen, W., Zhang, C., Li, Q., Zhang, W., Cao, L., Ye, J., 2015b. Preparation of titanium dioxide nano particle modified photocatalytic self-cleaning concrete. Journal of Cleaner Production 87(1), 762-765.

Shi, C., Li, Y., Zhang, J., Li, W., Chong, L., Xie, Z., 2016. Performance enhancement of recycled concrete aggregate - A review. Journal of Cleaner Production 112, 466-472.

Shi, Y., Song, Z., Jiang, L., 2016. Porous Concrete and Pervious Pavement. China Architecture

Publishing & Media Co., Ltd.

Standard for test method of mechanical properties on ordinary concrete. China Archicture & Building Press: Beijing, China, 2002; Volume GB/T 50081.

Tam, V.W.Y., 2008. Economic comparison of concrete recycling: A case study approach. Resources, Conservation and Recycling 52(5), 821-828.

Technical specification for pervious cement concrete pavement, China Archicture & Building Press: Beijing, China, 2009; Volume CJJ/T 135.

Test method of photocatalytic materials for air purification, China Standard Press: Beijing, China, 2009; Volume GB/T 23761.

United States Geological Survey. "Rainfall calculator, metric units: How much water falls during a storm?". Available via <https://water.usgs.gov/edu/activity-howmuchrain-metric.html>, accessed on 11 Jan 2018.

Wang, F., Yang, L., Wang, H., Yu, H., 2015. Facile preparation of photocatalytic exposed aggregate concrete with highly efficient and stable catalytic performance. *Chemical Engineering Journal* 264, 577-586.

Xiao, J., Li, J., Zhang, C., 2005. Mechanical properties of recycled aggregate concrete under uniaxial loading. Cem Concr Res 35(6), 1187-1194.

Xiao, J., Li, L., Shen, L., Poon, C.S., 2015. Compressive behaviour of recycled aggregate concrete under impact loading. Cem Concr Res 71, 46-55.

Xu, Y., 2015. The Corrosion Characteristics and Tensile Behavior of Reinforcement under Coupled Carbonation and Static Loading. Materials 2015, 8, 8561-8577.

Xu, Y., Chen, W., Jin, R., Shen, J., Smallbone, K., Yan, C., Hu, L., 2018. Experimental investigation of photocatalytic effects of concrete in air purification adopting entire concrete waste reuse model. J. Hazard. Mater. 353, 421-430.

Xu, Y., Sun, J., 2011. Influence of recycled aggregate on physical and mechanical properties of high performance recycled aggregate concrete, 2010 International Conference on Components, Packaging and Manufacturing Technology, ICCPMT 2010. Sanya, pp. 764-767.

Yang, J., Wang, G., Wang, D., Liu, C., Zhang, Z., 2017. A self-cleaning coating material of TiO2 porous microspheres/cement composite with high-efficient photocatalytic depollution performance. Materials Letters 200, 1-5.

Yang, L., Hakki, A., Zheng, L., Jones, M.R., Wang, F., Macphee, D.E., 2019. Photocatalytic concrete for NOx abatement: Supported TiO2 efficiencies and impacts. *Cement and Concrete Research* 116, 57-64.

Zhong, R., Wille, K., 2016. Compression response of normal and high strength pervious concrete. Constr Build Mater 109, 177-187.